JOURNAL OF
Materials
CHEMISTRY

Study of the iron/trimesic acid system for the hydrothermal synthesis of hybrid materials

Myriam Riou-Cavellec,*[a] Catherine Albinet,[a] Jean-Marc Grenèche[b] and Gérard Férey[a]

[a]*Institut Lavoisier, UMR CNRS 8637, Université de Versailles – St Quentin, 45 Avenue des Etats-Unis, 78035 Versailles Cedex, France. E-mail: cavellec@chimie.uvsq.fr; Fax: (33) (0) 1 39 25 43 58*
[b]*Laboratoire de Physique de l'Etat Condensé, UMR CNRS 6087, Université du Maine, Avenue O. Messiaen, 72085 Le Mans Cedex 9, France*

Received 20th May 2001, Accepted 4th October 2001
First published as an Advance Article on the web 25th October 2001

Two divalent iron trimesates were synthesized hydrothermally at 453 K for 72 hours under autogenous pressure using 1,3,5-benzenetricarboxylic acid (or trimesic acid, symbolized by BTC-H$_3$). The first one, [Fe(H$_2$O)$_4$(BTC-H$_2$)$_2$], is molecular and crystallizes in the monoclinic space group $P2_1/c$ (no. 14) with cell parameters at 293 K: $a = 5.1572(3)$ Å, $b = 13.0703(8)$ Å, $c = 15.2673(10)$ Å, $\beta = 97.209(2)°$, $Z = 2$. The second formulated [Fe$_3$(H$_2$O)$_{12}$(BTC)$_2$] is one-dimensional; it crystallizes in the monoclinic space group $C2$ (no. 5) with the following cell parameters at 293 K: $a = 17.5592(4)$ Å, $b = 12.9874(2)$ Å, $c = 6.6031(1)$, $\beta = 112.004(1)°$, $Z = 2$. Its structure is based on isolated undulating chains which are organized in such a way that they seem to built sheets. Mössbauer spectrometry confirmed the presence of two divalent iron sites in agreement with crystallographic results and also that this compound remains paramagnetic till 4.2 K.

Introduction

Recently, the syntheses of new three-dimensional hybrid open-framework materials including organic species[1] such as di- or tricarboxylic acids were mainly reported by Yaghi's,[2] Williams's[3] and Férey's[4] groups. To our knowledge, these compounds are essentially synthesized with 3d transition metal cations such as Co, Mn, Ni, Zn, Cu, Cd and 4f rare earths, coupled with either flexible (*e.g.* succinic acid, adipic acid) or rigid (*e.g.* trimesic acid, terephthalic acid) organic moieties. However, it seems that rigid species lead to more original open structures.

Until now, a unique iron succinate[5] isostructural with the Co succinate MIL-9[6] has been reported in the literature. In this paper, we report the first results obtained during the study of the iron/1,3,5-benzenetricarboxylic acid (or trimesic acid $C_9O_6H_6$ symbolized by BTC-H$_3$) system. Two iron(II)-based compounds were hydrothermally synthesized: the first one, [Fe(H$_2$O)$_4$(BTC-H$_2$)$_2$] (**1**), is molecular while the second one, formulated [Fe$_3$(H$_2$O)$_{12}$(BTC)$_2$] (**2**), displays one-dimensional character.

Experimental

Synthesis

Both compounds [Fe(H$_2$O)$_4$(BTC-H$_2$)$_2$] (**1**) and [Fe$_3$(H$_2$O)$_{12}$(BTC)$_2$] (**2**) were synthesized hydrothermally under autogenous pressure.

For (**1**), the reactants were $FeCl_2 \cdot 4H_2O$ (Aldrich), trimesic acid (Fluka, 97%), urea (Sigma-Aldrich) and water. The initial molar ratios were 1 : 1 : 1 : 80 (5 mL). The initial pH of the mixture was *ca.* 1, before heating. Compound (**1**) can also be obtained when the reactants are 1 $FeCl_2 \cdot 4H_2O$: 1.5 trimesic acid : 80 H_2O (5 mL), 1 mL of a KOH solution (10 mol L^{-1}) being used to increase the pH of the initial mixture to *ca.* 3–4. When neither urea nor KOH were added to the mixtures before heating, trimesic acid was recrystallized.

For (**2**), the reactants were Fe fine powder (Riedel de Haën), trimesic acid (Fluka, 97%) and water with initial molar ratios 1 : 1 : 200 (5 mL); the pH of the initial mixture was adjusted to *ca.* 3–4 using 0.3 mL of a KOH solution (10 mol L^{-1}).

Both mixtures were then introduced in 23 mL Teflon vessels and enclosed in Parr acid digestion bombs for heating at 453 K for 72 hours. We obtained in both cases a pasty inhomogenous and amorphous bulk with long rod-shaped crystals, colorless for (**1**) and green for (**2**). The pH, after heating, could not be estimated. Crystals of (**1**) and (**2**) were isolated from the pasty bulk and cleaned using an ultrasonic wave bath.

Analysis

Semi-quantitative EDX analyses (performed on a JEOL 5800 LV scanning microscope equipped with an Oxford Linkisis analyser) of both types of crystals confirmed that nitrogen and potassium are not present in (**1**) and (**2**).

Elemental analysis results (weight%) indicated for (**1**): Fe, 10.45 (theor.: 10.22), C, 38.75 (theor.: 39.55); for (**2**): Fe, 21.12 (theor.: 21.00), C, 27.58 (theor.: 27.07).

The experimental density measurements made using a Micromeritics 1330 Accupyc pycnometer are in good agreement with the theoretical values: 1.81(1) g cm^{-3} for (**1**) (theor.: 1.78 g cm^{-3}); 1.91(1) g cm^{-3} for (**2**) (theor.: 1.90 g cm^{-3}).

TGA measurements of compounds (**1**) and (**2**) were performed under O_2 gas flow (*ca.* 65 mL min^{-1}) using a TA-Instrument type 2050 analyser (Fig. 1). The heating rate was 5 °C min^{-1} from 30 to 600 °C. Both TGA curves of (**1**) and (**2**) display two distinct weight losses. The first weight loss corresponds to the dehydration of the compounds: for (**1**), from 70 to 230 °C, exp.: 15.1%, theor.: 13.2%; for (**2**), from 60 to 250 °C, exp.: 24.5%, theor.: 27%. The second weight loss was attributed to the calcination of the organic part of the structures: for (**1**), from 300 to 395 °C, exp.: 67.3%, theor.: 76.5%; for (**2**), from 300 to 375 °C, exp.: 45.6%, theor.: 51.9%. In both cases, the final residues were identified as Fe_2O_3 (by X-ray diffraction) so the whole experimental weight losses were in agreement with the theoretical ones: for (**1**), exp.: 82.4%, theor.: 85.3%; for (**2**), exp.: 70.1%, theor.: 69.9%.

Infrared spectra of (**1**) and (**2**) were measured from KBr pellets using a Nicolet Magma IR 550 device (4000–500 cm^{-1}).

DOI: 10.1039/b104495h

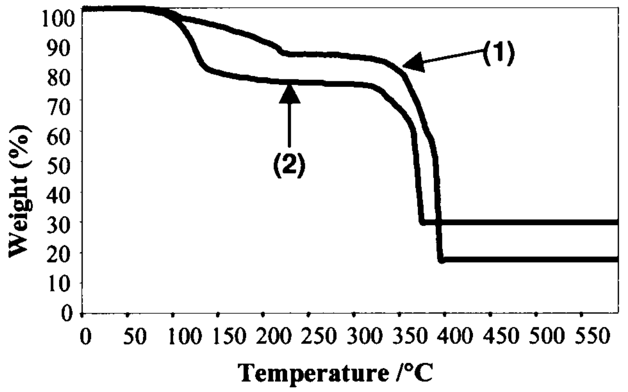

Fig. 1 TGA curves of compound (**1**) and compound (**2**) under O_2 gas flow.

Both spectra present a sharp band at 1624 cm^{-1} attributable to the presence of water molecules in the metal coordination spheres. For (**1**), we observed an absorption band at 1711 cm^{-1} which indicates $-CO_2H$ groups. For (**2**), the absence of bands in the range 1730–1690 cm^{-1} confirms the complete deprotonation of BTC-H_3 in the final compound.

Structural determination

The structures were determined from a single crystal X-ray diffraction study. Suitable single crystals of (**1**) ($0.860 \times 0.060 \times 0.020$ mm) and (**2**) ($0.180 \times 0.120 \times 0.120$ mm) were chosen and mounted on glass fibers. The data collections were performed on a SMART Siemens three-circle diffractometer equipped with a CCD detector (MoK_α monochromatized wavelength 0.71073 Å; 30 s and 120 s per frame for (**1**) and (**2**), respectively). The data reductions and Lorentz-polarization effect corrections were done using the SAINT program. An absorption correction specifically for the CCD detector was applied to all data using the SADABS program.[7] The structures were thus solved and refined with SHELX-TL crystallographic software package.[8]

The structures of compounds (**1**) and (**2**) were solved in centrosymmetric space group $P2_1/c$ (no. 14) and in non-centrosymmetric space group $C2$ (no. 5), respectively. Many atoms (Fe, O, C) were located from direct methods (TREF option), the remaining atoms (O, C) were deduced from Fourier difference map calculations. All the non-hydrogen atoms were refined with anisotropic thermal factors. For compound (**1**), all hydrogen atoms were localized from Fourier difference syntheses without applying any constraints; for compound (**2**), hydrogen atoms from aromatic CH groups were placed applying geometrical constraints (HFIX 43 option). At the final stage of refinements, the reliability factors are: for compound (**1**), $R_1(F) = 0.0514$, $wR_2(F^2) = 0.1111$ for 1581 reflections with $I > 2\sigma(I)$; for compound (**2**), $R_1(F) = 0.0578$, $wR_2(F^2) = 0.1540$ for 2743 reflections with $I > 2\sigma(I)$.

Table 1 Crystallochemical data for (**1**) and (**2**)

	(**1**)	(**2**)
Chemical formula	$[Fe(H_2O)_4(C_9O_6H_5)_2]$	$[Fe_3(H_2O)_{12}(C_9O_6H_3)_2]$
Formula weight/g mol^{-1}	546.18	797.54
Crystal system	Monoclinic	Monoclinic
Space group	$P2_1/c$ (no. 14)	$C2$ (no. 5)
Cell parameters/Å, °	$a = 5.1572(3)$ $b = 13.0703(8)$ $c = 15.2673(10)$ $\beta = 97.209(2)$	$a = 17.5592(4)$ $b = 12.9874(2)$ $c = 6.6031(1)$ $\beta = 112.004(1)$
Volume/$Å^3$, Z	1020.97(11), 2	1396.14(4), 2
Absorption coefficient/cm^{-1}	8.28	16.44
Reflections collected	3564	4811
Independent reflections	2331 [R(int) = 0.0376]	2884 [R(int) = 0.0295]
Data/restraints/parameters	2331/0/197	2884/1/208
Final R indices [$I > 2\sigma(I)$]	$R_1(F_o) = 0.0514$, $wR_2(F_o^2) = 0.1111$	$R_1(F_o) = 0.0578$ $wR_2(F_o^2) = 0.1540$
Largest diff. peak and hole/e^- $Å^{-3}$	0.624 and −0.393	0.925 and −1.454

The conditions of data collection for (**1**) and (**2**) are summarized in Table 1. Atomic coordinates, principal bond lengths and angles characteristic of compounds (**1**) and (**2**) are listed in Tables 2 and 3.

Table 2 Atomic coordinates ($\times 10^4$, $\times 10^3$ for hydrogen atoms) and equivalent isotropic displacement parameters ($Å^2 \times 10^3$)

	x	y	z	U(eq)
For compound (1):				
Fe(1)	0	5000	0	21(1)
O(1)^{w}	−1426(5)	3935(2)	890(2)	32(1)
O(2)^{w}	3263(5)	5297(2)	969(2)	29(1)
O(3)	−2142(4)	6166(2)	545(2)	25(1)
O(4)^{h}	5447(5)	7055(2)	2524(2)	41(1)
O(5)	−6631(5)	3660(2)	2114(2)	33(1)
O(6)	−4679(4)	7350(2)	−176(2)	32(1)
O(7)	9796(5)	6518(2)	3531(2)	40(1)
O(8)^{h}	3376(5)	5885(2)	4292(2)	48(1)
C(1)	−5112(6)	3060(3)	2511(2)	24(1)
C(2)	−2713(6)	3372(2)	3106(2)	23(1)
C(3)^{c}	−2027(6)	4405(3)	3195(2)	25(1)
C(4)^{c}	−1167(6)	2632(3)	3572(2)	22(1)
C(5)^{c}	1716(6)	3940(3)	4223(2)	24(1)
C(6)	−2735(6)	7094(2)	361(2)	22(1)
C(7)	1062(6)	2911(2)	4144(2)	20(1)
C(8)	214(6)	4683(2)	3741(2)	23(1)
C(9)	1060(7)	5791(3)	3839(2)	27(1)
H(1a)^{w}	−271(11)	350(4)	69(4)	78(18)
H(1b)^{w}	−24(9)	369(3)	124(3)	44(13)
H(2a)^{w}	344(7)	486(3)	126(3)	21(12)
H(2b)^{w}	469(9)	546(4)	90(3)	60(17)
H(4)^{h}	692(11)	688(4)	289(4)	79(17)
H(8)^{h}	385(9)	649(4)	440(3)	48(13)
H(3)^{c}	−295(7)	489(3)	289(3)	29(10)
H(4)^{c}	−160(7)	195(3)	350(3)	35(11)
H(5)^{c}	330(7)	411(3)	458(3)	20(9)
For compound (2):				
Fe(1)	7412(1)	7638(1)	7139(1)	24(1)
Fe(2)	0	488(1)	0	27(1)
O(1)^{w}	8218(2)	8711(3)	6536(7)	29(1)
O(2)^{w}	859(3)	−470(5)	9612(8)	52(2)
O(3)	649(2)	1954(3)	186(7)	29(1)
O(4)^{w}	6586(2)	6515(4)	7521(7)	32(1)
O(5)	8436(2)	6697(3)	8574(7)	29(1)
O(6)^{w}	9447(3)	457(4)	6487(7)	37(1)
O(7)	6456(2)	8705(3)	5923(7)	30(1)
O(8)^{w}	7644(3)	8318(4)	344(7)	34(1)
O(9)^{w}	7204(2)	7019(4)	3888(7)	38(1)
O(10)	5682(3)	3523(4)	5608(8)	38(1)
O(11)	7846(2)	5252(3)	9077(8)	34(1)
O(12)	7140(2)	136(3)	5824(8)	32(1)
C(1A)^{c}	9272(3)	4133(4)	9628(8)	24(1)
C(2A)	0	3586(6)	0	23(1)
C(3A)	9261(3)	5201(4)	9567(8)	24(1)
C(4A)^{c}	0	5742(6)	0	22(1)
C(5A)	8456(3)	5772(4)	9041(7)	22(1)
C(6A)	0	2461(7)	0	28(2)
C(7B)	5000	1892(6)	5000	21(1)
C(8B)^{c}	5728(3)	1347(4)	5377(8)	23(1)
C(9B)	5000	3041(7)	5000	29(2)
C(10B)	5733(3)	275(4)	5377(8)	23(1)
C(11B)^{c}	5000	9756(6)	5000	22(1)
C(12B)	6502(3)	9668(4)	5753(8)	24(1)
H(1A)^{c}	879(1)	377(1)	942(1)	29
H(4A)^{c}	0	646(1)	0	27
H(8B)^{c}	621(1)	171(1)	563(1)	27
H(11B)^{c}	500	904(1)	500	27

U(eq) is defined as one third of the trace of the orthogonalized U_{ij} tensor. w, h and c mean that the designed atom belongs to a terminal water molecule, a hydroxyl group within a carboxylic group or an aromatic C–H bond, respectively.

Table 3 Principal bond lengths [Å] and angles [°]

For compound (1):			
Within $[Fe(H_2O)_4O_2]$ octahedra:			
Fe(1)–O(3)	2.114(2) × 2		
Fe(1)–O(2)^w	2.132(3) × 2		
Fe(1)–O(1)^w	2.139(3) × 2		
Within BTC-H_2 moiety:			
C(1)–C(2)	1.496(4)	C(1)–O(4)^h	1.325(4)
C(2)–C(3)	1.399(5)	C(1)–O(5)	1.215(4)
C(2)–C(4)	1.391(4)	O(4)–C(1)–O(5)	123.2(3)
C(3)–C(8)	1.387(4)	C(6)–O(3)	1.273(4)
C(4)–C(7)	1.402(4)	C(6)–O(6)	1.259(4)
C(7)–C(5)	1.387(5)	O(3)–C(6)–O(6)	123.1(3)
C(8)–C(5)	1.393(4)	C(9)–O(7)	1.213(4)
C(7)–C(6)	1.514(4)	C(9)–O(8)^h	1.309(4)
C(8)–C(9)	1.515(5)	O(7)–C(9)–O(8)	122.9(3)
For compound (2):			
Within $[Fe(H_2O)_4O_2]$ octahedra:			
Fe(1)–O(5)	2.084(4)	Fe(2)–O(2)^w	2.045(5) × 2
Fe(1)–O(7)	2.092(4)	Fe(2)–O(6)^w	2.154(4) × 2
Fe(1)–O(1)^w	2.127(4)	Fe(2)–O(3)	2.199(4) × 2
Fe(1)–O(4)^w	2.137(4)		
Fe(1)–O(8)^w	2.186(4)		
Fe(1)–O(9)^w	2.191(4)		
Within BTC (A) organic moiety:			
C(6A)–C(2A)	1.46(1)	C(6A)–O(3)	1.281(6) × 2
C(2A)–C(1A)	1.401(6) × 2	O(3)–C(6A)–O(3)	118.2(7)
C(1A)–C(3A)	1.387(8) × 2	C(5A)–O(5)	1.238(7)
C(3A)–C(4A)	1.408(6) × 2	C(5A)–O(11)	1.273(6)
C(3A)–C(5A)	1.517(7) × 2	O(5)–C(5A)–O(11)	125.0(5)
Within BTC (B) organic moiety:			
C(9B)–C(7B)	1.49(1)	C(9B)–O(10)	1.275(6) × 2
C(7B)–C(8B)	1.399(6) × 2	O(10)–C(9B)–O(10)	121.3(8)
C(8B)–C(10B)	1.391(8) × 2	C(12B)–O(7)	1.261(7)
C(10B)–C(11B)	1.390(6) × 2	C(12B)–O(12)	1.259(6)
C(10B)–C(12B)	1.503(7) × 2	O(7)–C(12B)–O(12)	124.2(5)

w is for a terminal water molecule, h for a carboxylic group.

CCDC reference numbers 171986 and 171987. See http://www.rsc.org/suppdata/jm/b1/b104495h/ for crystallographic files in CIF or other electronic format.

Magnetic measurements and ^{57}Fe Mössbauer spectrometry

The magnetisation M of (**2**) was measured with a Quantum Design SQUID magnetometer. $M(H)$ values measured between 0 and 5.5 T at different temperatures (from 4.5 K to 290 K), and also zero field cooled and field cooled $M(T)$ curves at $H = 0.01$ T are reported.

Mössbauer experiments were carried out at 300, 77 and 4.2 K by means of a bath cryostat, using a constant acceleration spectrometer and a Co source diffused into a Rh matrix. The values of the isomer shift are quoted relative to that of α-Fe foil at 300 K. The hyperfine parameters were refined using a least-square fitting procedure in MOSFIT program.[9]

Results and discussion

The structure of $[Fe(H_2O)_4(C_9O_6H_5)_2]$ (**1**) is molecular (Fig. 2). It is built on units constituted of a $[Fe^{II}O_2(H_2O)_4]$ octahedron bonded to two $[BTC\text{-}H_2]^-$ organic groups *via* O(3) atoms (see Tables 2 and 3). Both O(1)^w and O(2)^w vertices are actually terminal water molecules; O(1)^w is linked to H(1a)^w and H(1b)^w atoms, O(2)^w to H(2a)^w and H(2b)^w atoms. Valence bond calculations[10] are in agreement with iron in the oxidation state +II (2.068 v.u.); within the octahedron, bond lengths are in the range 2.114 to 2.139 Å. In compound (**1**), the trimesic species BTC-H_3 is partly deprotonated and becomes a $[BTC\text{-}H_2]^-$ moiety. Within the two remaining carboxylic groups, the oxygen atoms O(4)^h and O(8)^h are bonded respectively to H(4)^h and H(8)^h; the third group (C(6), O(6), O(3)) is deprotonated. This carboxylate group is involved in strong hydrogen bonds (see Table 4) *via* the O(6) atom: O(6)···H(8)^h = 1.773 Å, O(6)···H(1a)^w = 1.845 Å as well as the O(7) atom from one carboxylic group: O(7)···H(4)^h = 1.741 Å; these hydrogen bonds occur between adjacent BTC-H_2 units and lead to the formation of pseudo sheets of $[BTC\text{-}H_2]^-$ moieties between which are located the iron octahedra (Fig. 3 and 4). Other important hydrogen bonds exist between O(3) and O(5) atoms belonging to the $[BTC\text{-}H_2]^-$ moieties and the hydrogen atoms of terminal water molecules located on the 'intercalated' iron octahedra: O(3)···H(2b)^w = 2.011 Å, O(5)···H(2a)^w = 2.05 Å, O(5)···H(1b)^w = 2.151 Å. This set of strong hydrogen bonds leads to a pseudo three-dimensional structure displaying free rectangular channels (Fig. 4).

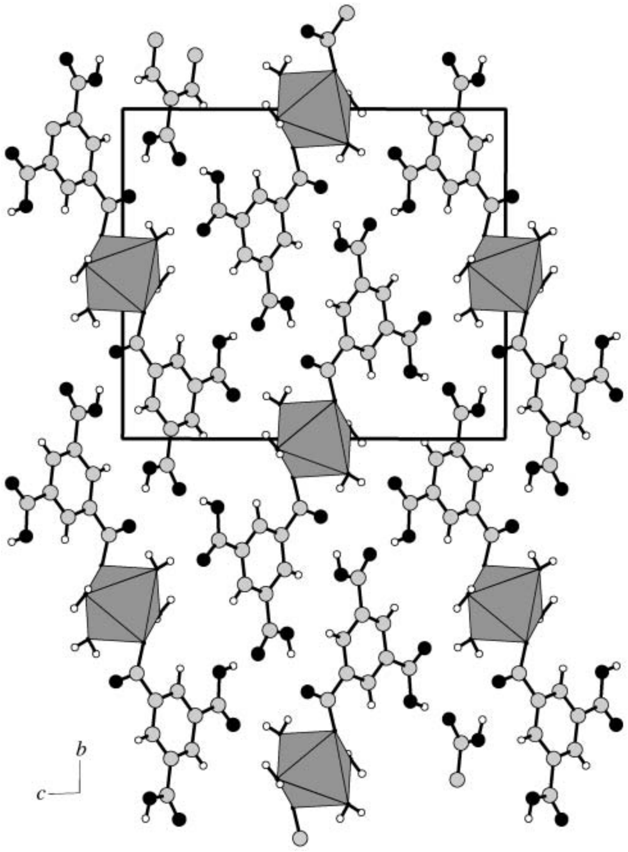

Fig. 2 Projection of the structure of compound (**1**) along [100].

The Mössbauer spectrum recorded at 77 K from compound (**1**) exhibits a doublet with well resolved lines which is well reproduced by using a single quadrupolar component, consistent with a unique Fe environment. The refined parameters are typical of high-spin Fe^{2+} in octahedral coordination: IS = 1.38 mm s^{-1}, FWHM = 0.25 mm s^{-1} and QS = 3.86 mm s^{-1} (see Table 5 for definitions).

The structure of the second compound $[Fe_3(H_2O)_{12}(C_9O_6H_3)_2]$ (**2**) is one-dimensional (Fig. 5a). It is based on zig-zag chains built up from the connection of isolated

Table 4 Principal O···H–O angles (degrees) for compound (**1**)

O(6)···H(8)^h–O(8)^h	166.69
O(6)···H(1a)^w–O(1)^w	175.18
O(7)···H(4)^h–O(4)^h	176.86
O(3)···H(2b)^w–O(2)^w	165.20
O(5)···H(2a)^w–O(2)^w	171.18
O(5)···H(1b)^w–O(1)^w	157.86

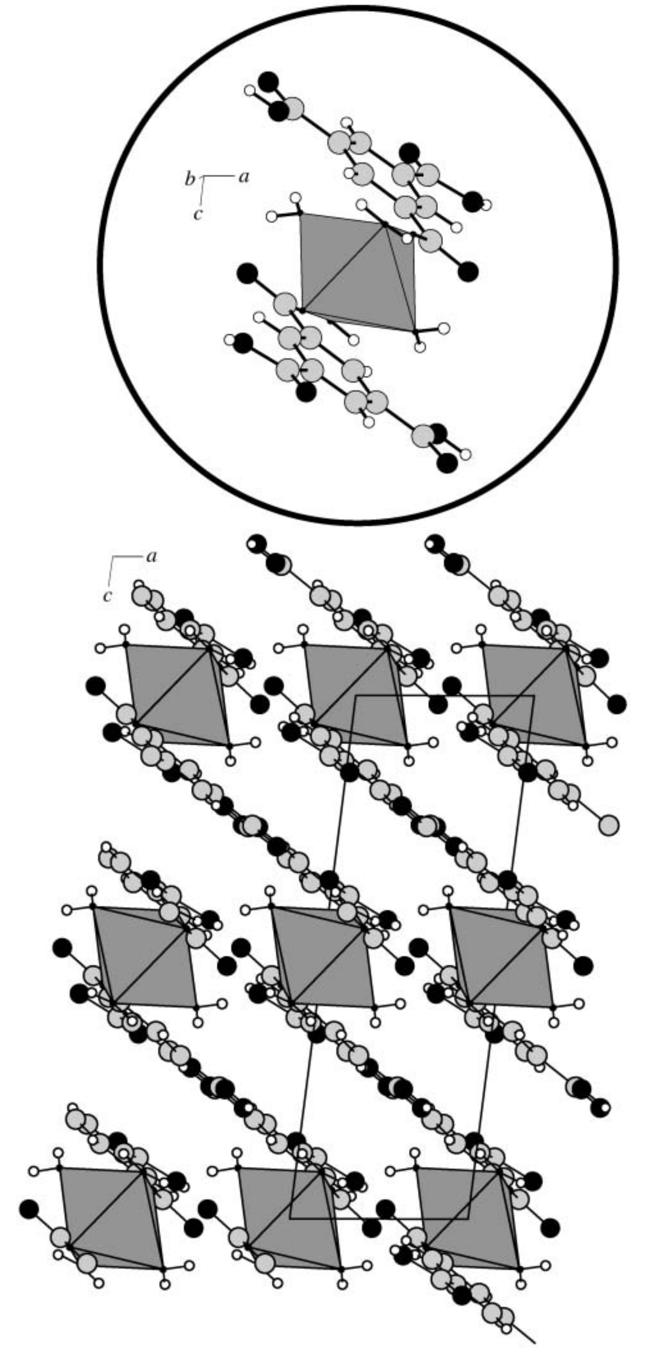

Fig. 3 Projection of the structure of compound (**1**) along [010] and the formation of organic sheets.

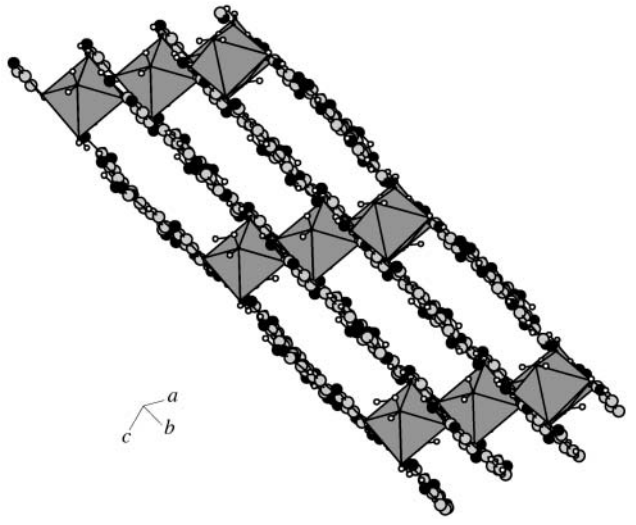

Fig. 4 View of the pseudo 3D structure of compound (**1**) displaying rectangular empty channels.

Table 5 Refined values of hyperfine Mössbauer parameters

T/K	Component Γ_i	IS/ mm s^{-1} $\pm$0.02	FWHM/ mm s^{-1} $\pm$0.02	QS/ mm s^{-1} $\pm$0.02	% $\pm$2
300	Γ_1	1.22	0.27	2.06	68
	Γ_2	1.21	0.31	2.84	32
77	Γ_1	1.34	0.28	3.06	66
	Γ_2	1.33	0.26	3.51	34
4.2	Γ_1	1.35	0.33	3.15	66
	Γ_2	1.34	0.31	3.54	34

IS: isomer shift; FWHM: linewidth at halfheight; QS: quadrupolar splitting; %: ratio of each component.

$[Fe(H_2O)_4O_2]$ octahedra by two different rigid trimesate groups A and B (BTC^{3-} ions) (Tables 2 and 3). Fe(1) octahedra are bonded to trimesates A and B *via* O(5) and O(7) vertices, respectively: O(5) and O(7) ligands are in *trans* positions on the Fe(1) octahedra (see Fig. 5a). As for Fe(2), it is chelated by one carboxylate group (C(6A), O(3), O(3) group) from trimesate A inducing a real distortion[11] Δ of the octahedron (short O(3)–O(3) edge = 2.198 Å): $\Delta \times 10^4 = 3.74$ for $[Fe(1)(H_2O)_4O_2]$ octahedron, $\Delta \times 10^4 = 9.18$ for $[Fe(2)(H_2O)_4O_2]$ octahedron. Bond valence calculations confirmed the oxidation state +II for Fe(1) (2.036 v.u.) and Fe(2) (2.074 v.u.); Fe–O bond lengths ranged from 2.084–2.191 Å within the Fe(1) octahedron and 2.045–2.199 Å within the Fe(2) octahedron (Table 3). These calculations are also in agreement with IR results about the presence of terminal water molecules on iron polyhedra: $O(1)^w$, $O(4)^w$, $O(8)^w$ and $O(9)^w$ on the Fe(1) octahedron; $O(2)^w$, $O(6)^w$ on the Fe(2) octahedron. All carboxylate groups are either bonding or chelating iron except a non-bonded carboxylate group in trimesate B (C(9B), O(10), O(10) group) (Fig. 5a).

Even if the hydrogen atoms from water molecules were not located in (**2**), it is likely that the zig-zag chains are connected together by hydrogen bonds between terminal water molecules located on iron octahedra, in agreement with the short distance $O(1)^w \cdots O(2)^w = 2.671$ Å (represented by dotted lines in Fig. 5a). This leads to the formation of pseudo-layers parallel to the *ab* plane. These pseudo-layers stack in the [001] direction in a staggered manner (Fig. 5b). The layers are also held together by quite strong hydrogen bonds; two significant short O···O bonds are also represented in Fig. 5b: $O(11) \cdots O(8)^w = 2.728$ Å, $O(10) \cdots O(1)^w = 2.802$ Å. As for compound (**1**), compound (**2**) presents a pseudo 3D structure.

According to Mössbauer spectrometry, compound (**2**) remains paramagnetic at 4.2 K; this is in agreement with the presence of 'isolated' iron polyhedra in the structure. The Mössbauer spectra recorded at 300, 77 and 4.2 K (Fig. 6) exhibit a doublet with better resolved lines at 300 K. These spectra are well reproduced by using only two quadrupolar components Γ_i without any constraints. The theoretical expected proportion for each component is 2/3 (for Fe(1)) and 1/3 (for Fe(2)) according to the crystallographic data. The obtained refined parameters are listed in Table 5 and their values are in good agreement with those expected. Moreover, the two isomer shift values (IS) are consistent with high-spin Fe^{2+} in octahedral coordination; the thermal evolution of quadrupolar splitting (QS) is also characteristic of iron in oxidation state +II. The two quadrupolar components Γ_1 and Γ_2 can be easily attributed to iron sites according to their respective proportions: Γ_1 corresponds to Fe(1) sites and Γ_2 to Fe(2) sites. This attribution is also in agreement with the observed QS values:

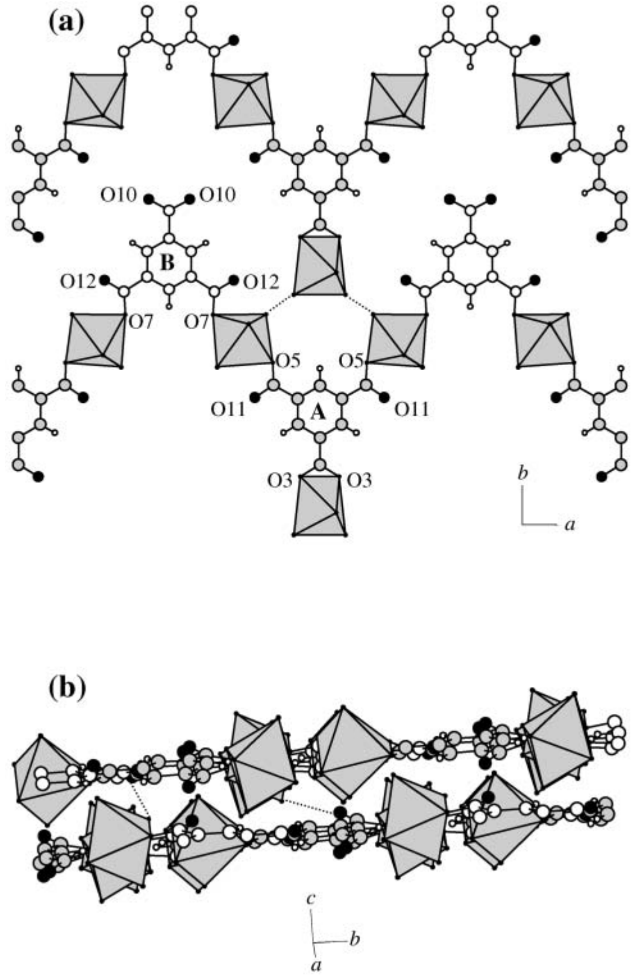

Fig. 5 (a) Zig-zag chains leading to pseudo sheets parallel to the *ab* plane; (b) stacking of two consecutive sheets along [001]. Most important intra- and inter-sheet hydrogen bonds are represented by dotted lines.

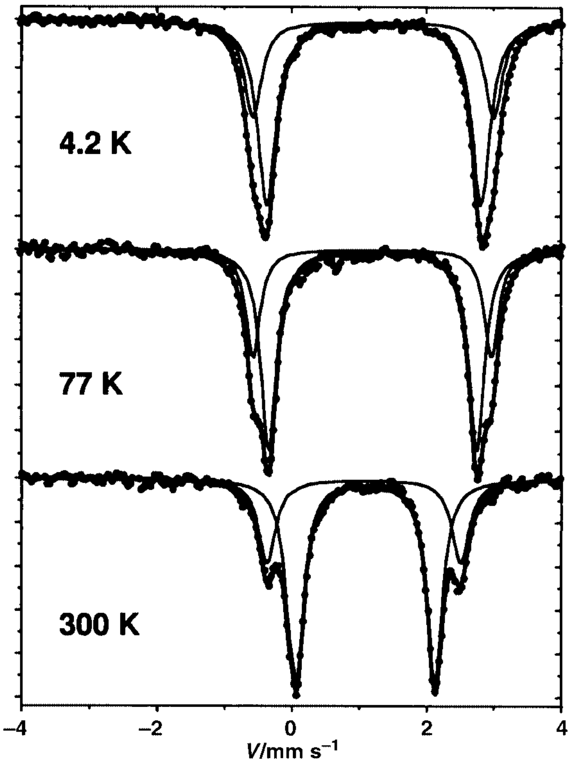

Fig. 6 Fits of Mössbauer spectra of compound (**2**) at 300, 77 and 4.2 K with two distinct quadrupolar components.

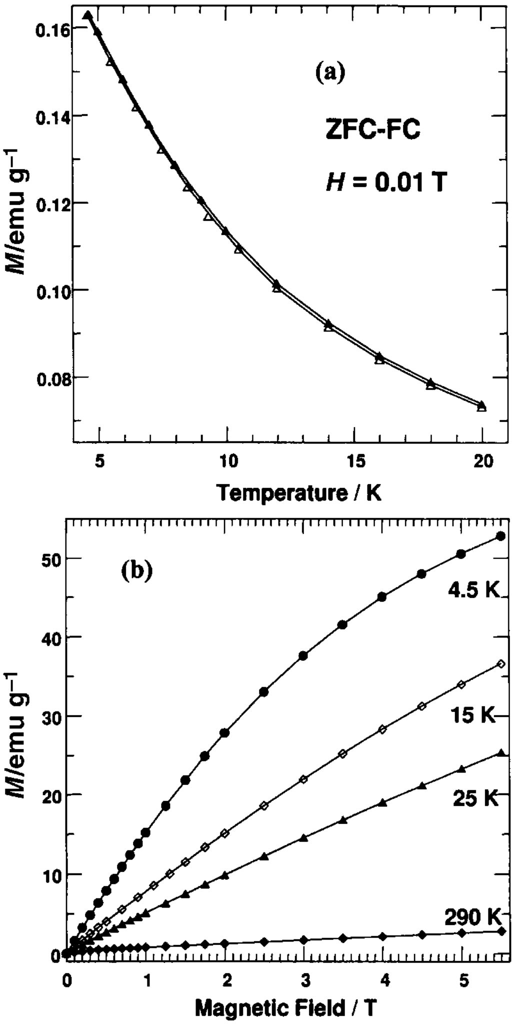

Fig. 7 (a) ZFC and FC (magnetic field $H = 0.01$ T) magnetization curves *versus* temperature (between 5 and 20 K). (b) Magnetization M *versus* magnetic field H for compound (**2**). The line joining the points is just a guide for the eyes.

the larger the distortion of the octahedron, the higher the QS value.[12]

However, despite this paramagnetism at 4.2 K, which is also confirmed by ZFC–FC magnetization curves (Fig. 7a), the $M(H)$ curves indicate pretransitional order with a beginning of curvature on the $M(H)$ curves at low temperatures (Fig. 7b) (note that the residual curvature observed at 290 K is probably due to a small amount of magnetic fine metallic iron particles arising from the synthesis method and that we could not extract). This low-temperature curvature suggests a likely ferrimagnetic order, below 4.2 K, in agreement with the different multiplicities on the two Fe^{2+} sites. Indeed, Fe^{2+} cations are on 2a and 4c crystallographic Wyckoff sites. Fe^{2+}(2a) corresponds to the dangling octahedron (labelled Fe(2)) whereas Fe^{2+}(4c) is linked to two *trans* trimesate groups (labelled Fe(1)). If the spins on 4c sites are up, and assuming that Fe^{2+}–Fe^{2+} ($3d^6$) couplings are antiferromagnetic,[13] spins on 2a sites are down. The magnetic resultant is therefore not zero and ferrimagnetism probably appears at very low temperatures.

Conclusion

Both compounds described in this paper display pseudo 3D structures *via* the existence of complex hydrogen bond networks; these latter have also been observed in rare earth[14] and cobalt trimesate complexes.[15–16] As the title compounds can be synthesized with cobalt cations, an interesting perspective is to develop the hydrothermal synthesis of open-framework Fe–Co trimesates; this is currently in progress and the structure of a new mixed 3D phase will be published elsewhere.

Acknowledgement

The authors thank Dr Marc Noguès (LMOV, University of Versailles-St Quentin) for magnetization measurements.

References

1 B. F. Abrahams, B. F. Hoskins, D. M. Michail and R. Robson, *Nature*, 1994, **369**, 727.
2 O. M. Yaghi, E. C. Davis, G. Li and H. Li, *J. Am. Chem. Soc.*, 1997, **119**, 2861; H. Li, M. Eddaoudi, M. O'Keeffe and O. M. Yaghi, *Nature*, 1999, **402**, 276.
3 S. S.-Y. Chui, S. M.-F. Lo, J. P. H. Charmant, A. G. Orpen and I. D. Williams, *Science*, 1999, **283**, 1148.
4 F. Serpaggi and G. Férey, *J. Mater. Chem.*, 1998, **8**, 2737; A. K. Cheetham, G. Férey and T. Loiseau, *Angew. Chem., Int. Ed.*, 1999, **38**, 3268.
5 Y. Kim and D.-Y. Jung, *Bull. Korean Chem. Soc.*, 1999, **20**, 827.
6 C. Livage, C. Egger, M. Nogues and G. Férey, *J. Mater. Chem.*, 1998, **8**, 2743.
7 G. Sheldrick, SADABS program: Siemens Area Detector Absorption Corrections, unpublished.
8 G. Sheldrick, SHELX-TL software package (including SAINT program), University of Göttingen, Germany, 1994.
9 J. Teillet and F. Varret, MOSFIT Program, unpublished.
10 N. E. Brese and M. O'Keeffe, *Acta Crystallogr., Sect. B*, 1991, **47**, 192.
11 R. D. Shannon, *Acta Crystallogr., Sect. A*, 1976, **32**, 751.
12 N. N. Greenwood and T. C. Gibb, *Mössbauer spectroscopy*, Chapman and Hall Ltd., London, 1971.
13 J. B. Goodenough, in *Magnetism and the Chemical Bond*, Interscience, New York, 1963.
14 C. Daiguebonne, O. Guilloa, Y. Gérault, A. Lecerf and K. Boubekeur, *Inorg. Chim. Acta*, 1999, **284**, 139.
15 N. Guillou, C. Livage, J. Marrot and G. Férey, *Acta Crystallogr., Sect. C*, 2000, **56**, 1427.
16 O. M. Yaghi, H. Li and T. L. Groy, *J. Am. Chem. Soc.*, 1996, **118**, 9096.